

## Supplementary Information for

Inhibition of soluble epoxide hydrolase attenuates a high fat diet-mediated renal injury by activating PAX2 and AMPK

Ying Luo, Ming-Yu Wu, Bing-Qing Deng, Jian Huang, Sung Hee Hwang, Meng-Yuan Li, Chun-Yu Zhou, Qian-Yun Zhang, Hai-Bo Yu, Da-Ke Zhao, Guodong Zhang, Ling Qin, Ai Peng, Bruce D Hammock, and Jun-Yan Liu

Corresponding author: Bruce D. Hammock or Jun-Yan Liu

Email: [bdhammock@ucdavis.edu](mailto:bdhammock@ucdavis.edu) or [jyliu@tongji.edu.cn](mailto:jyliu@tongji.edu.cn)

### **This PDF file includes:**

Supplementary text

Figs. S1 to S14

Tables S1 to S5

References for SI reference citations

## Supplementary Information Appendix (*SI Appendix*)

### Materials and Methods

#### Chemicals and reagents

9(10)-EpOME, 12(13)-EpOME, 14,15-DHET, 14(15)-, 11(12)-, 8(9)-, 5(6)-EET, and 14,15-EE-5(Z)E, as well as the antibody for sEH were purchased from a local distributor of Cayman Chemical (Ann Arbor, MI) in Shanghai, China. Creatinine was purchased from a branch of MedChemExpress in Shanghai, China while the urea and urea-1, 3-<sup>15</sup>N<sub>2</sub> were purchased from a local distributor of Sigma-Aldrich (St. Louis, MO) in Shanghai, China. Creatinine (N-methyl-d<sub>3</sub>) was purchased from a local distributor of Cambridge Isotope Laboratories Inc. (Andover, MA). 1-trifluoromethoxyphenyl-3-(1-propionylpiperidin-4-yl)urea (TPPU) was synthesized by the Hammock Laboratory according to the previously reported procedure (1). The compound was characterized by thin layer chromatography (TLC), high performance liquid chromatography-mass spectrometry (HPLC-MS), and nuclear magnetic resonance (NMR). A Periodic Acid-Schiff (PAS) kit (#20061487) was purchased from Shanghai Hongqiao Lexiang Institute of Biomedical Products (Shanghai, China). The primers for quantitative real time PCR were prepared by Shanghai Generay Biotech Co. Ltd. (Shanghai, China) with the sequences detailed in *SI Appendix Table S3*. The antibodies for p-Ampk $\alpha$  (Thr172), and Pax2 were purchased from the local distributors of Cell Signaling Technology (Beverly, MA) and Abcam (Cambridge, MA), respectively. The antibody for p-Pax2 (Ser393) was purchased from a local distributor of Invitrogen, Thermo Fisher Scientific (Waltham, MA). The murine renal mesangial cells (mRMCs, SV40 MES13) and the associated cell culture medium DMEM (Dulbecco's Modified Eagle Medium) high glucose +23.75% F-12+5% FBS+14mM HEPES+1% penicillin-streptomycin were purchased from Shanghai Zhong Qiao Xin Zhou Biotechnology Co., Ltd.

(Shanghai, China). Primary murine renal tubular epithelial cells (mRTECs) were purchased from Shanghai Suer Biotech Co Ltd NE-PER nuclear and cytoplasmic extraction reagents (#78833) were purchased from a local distributor of Thermo Fisher Scientific (Rockford, IL).

### **Animal protocols**

All animal experiments were performed according to the protocols approved by the Animal Use and Care Committee of Shanghai Tenth People's Hospital, Tongji University School of Medicine. Male mice (C57BL/6, 7-week old) were purchased from Shanghai Lab Animal Research Center (Shanghai, China). The mice were housed in a temperature consistent animal room with a 12-hour light/dark cycle and freely access to food and water *ad lib*. A HFD (60 kcal% fat, D12492J) and the control diet (CTD, 10 kcal% fat, D12450J) were purchased from Research Diets, Inc. (New Brunswick, NJ).

In the first experiment, mice were randomly assigned into six groups (N = 11-12). After 1-week accommodation, the animals in three groups were fed with a HFD and the others fed on a CTD for 2, 4, and 8 weeks, respectively, as described in *SI Appendix* Table S1. The body mass for each animal was recorded prior to the treatment start and then weekly. The mice were anesthetized by intraperitoneal (*i.p.*) injection of chloral hydrate [3.5% (m/m) in saline, 0.35 mL per mouse] prior to sacrifice. The blood was collected for separation of plasma according to the protocol described previously (2). Both kidneys were collected. After the mass was recorded, the left one and a half of the right one were flash frozen in liquid nitrogen for qPCR, western blot, and LSMs analyses while the remaining of right one was fixed in 10% buffered formalin for histological examination. The one and half kidneys and the plasma were stored under -80°C until analysis. The right tibia was removed, and the length was recorded by using a slide caliper. The length was used to normalize the renal mass.

In the second experiment, mice were assigned into three groups at random (N = 10). The mice in group 1 were fed on a CTD. The mice in group 2 were fed on a HFD and those in group 3 were fed on a HFD with TPPU provided in drinking water at 10 mg/L. The TPPU was dissolved in polyethylene glycerol (PEG400) and then added to drinking water with stirring to give a solution of TPPU in drinking water with 0.2% PEG400 (v/v). The drinking water with 0.2% PEG400 (v/v) was served as a control. After 8 weeks treatment, the animals were sacrificed as the protocol described above.

### **Histological Examination**

The renal tissues were prepared for microscopic analysis with PAS stain following previously reported protocol (3).

### **Measurement of plasma levels of creatinine and urea**

The plasma levels of creatinine were measured on a LC-MS/MS instrument following the method reported previously by Liu *et al.* (4) The plasma levels of urea were measured together with creatinine used urea-<sup>13</sup>C<sub>1</sub> as the internal standard. The MRM modes used for monitoring urea and its internal standard were 60.9/44.1 and 62.1/45.1, respectively. The accuracy and precision of urea were validated to be acceptable.

### **Measurement of plasma level of glucose**

The thawed plasma (2 uL) was used for the measurement of plasma glucose by a Bayer Contour blood glucose meter (Bayer HealthCare LLC.) equipped with the associated test strips.

### **Measurement of renal levels of lipid signaling molecules**

The LSMs were extracted from the renal cortex according to the protocols reported by Wang *et al.* (5). The LSMs were quantitatively analyzed on an Agilent 1260 coupled with an AB Sciex QTrap 6500 according to the method reported previously (6).

## Plasmid construction

Pax2 small interfering (si)RNA (Sense: 5'- CACCGCATCAGAGCACATCAAATCATTCAAG AGATGATTTGATGTGCTCTGATGCTTTTTTTG-3'), Ampk small interfering (si)RNA (Sense: 5'- CACCGCACGAGTTGACCGGACATAATTCAAGAGATTATGTCCGGTCAACTCGTG CTTTTTTG-3') and a negative control (Sense: 5'- CACCGTTCTCCGAACGTGTCACGTTTC AAGAGAACGTGACACGTTTCGGAGAATTTTTTTG -3', a scrambled sequence with no match to any known gene) were selected according to the full-length cDNA of mouse *Pax2* and *Ampk*. siRNA sequences were synthesized and inserted into the pGPU6/GFP/Neo vector by Shanghai GenePharma Co., Ltd (Shanghai, China), which were named *shPax2*, *shAmpk*, and *shCon*, respectively.

The eukaryotic expression vector pIRES2-EGFP encoding the mouse *Pax2* and *Ampk $\alpha$ 1* was synthesized by GENERay Biothechnology (Shanghai, China). The empty eukaryotic expression vector pIRES2-EGFP was used as the expression control, which we named *oeCon*.

The CDS of *Pax2*: GenBank™ accession number NM\_011037.4

```
a tggaaacagcg tgcaagtcca gcagtcctga agttgagttt gagaggcgac acggcggcgg cggccgcgtt gctcccgtc
ctctgcctcc cgatggatat gcaactgcaa gcagaccct tctccgcgat gcaccaggc cacgggggtg tgaaccagct
cgggggggtg tttgtgaac gccggccct acccgactg gtaggcagc gcatcgtgga gctggccac cagggtgtgc
ggcctgtga catctcccgg cagctgcggg tcagccatgg ctgtgtcagc aaaatcctgg gcaggtacta cgagactggc
agcatcaagc ccggagtgat tgggtgctcc aagcccaagg tggcaacgcc caaagtggg gacaagattg ccgaatacaa
gcgacagaac ccgactatgt tcgcctggga gatccgtgac aggtgctag ccgagggcat ctgcgataat gacacagttc
ccagtgctc atccatcaac aggatcatcc ggaccaaagt tcagcagcct tccaccaa cgccggatgg ggcagggaca
ggagtgactg cccccggcca caccatcgtt cccagcacgg cctcccctcc tgtttccagc gecttaacg acccagtggg
atcctactcc atcaacggga tcttgggat tctcgtctc aacggtgaga agaggaaacg cgaggaagtc gaggtataca
```

ctgatcctgc ccacattaga ggaggtggag gtttacctt ggtctggact ttaagagatg tgtctgaggg ctctgtcct  
aatggagact cccagagtgg tgtggacagt ttgcggaagc acctgcgagc cgacacctc acccagcagc agctggaagc  
tctggatcga gtctttgagc gtccttcta tcccgatgtc ttccaggcat cagagcacat caaatcagaa caggggaatg  
aatactctct cccagccctg acccctgggc ttgatgaagt caagtcagc ctatctgcat cggccaacc tgagctgggc  
agcaatgtgt caggcacaca gacgtacccc gttgtgaccg gtcgtgatat gacgagcacc actctacctg gttaccccc  
tcattgtccc cccactggcc agggaagcta ccctacctc accctggcag gaatggtgcc tgtgccccc cccggggctc  
cgcccctgcc gctgctgccg ctgcctatga ccgccactag ttaccgccc gaccacatca agcttcaggc agacagcttc  
ggcctccaca tcgtccccgt ctga. We named *oePax2*.

The CDS of *Ampk $\alpha$ 1*: GenBank<sup>TM</sup> accession number NM\_001013385.3

at ggcagactc agttcttga gaaagatggc gacggccgag aagcagaagc acgacgggcg ggtgaagatc ggccactaca  
tctgggggga cacgcttggc gtcggcacct tcgggaaagt gaaggtgggc aagcacgagt tgaccggaca taaagtggc  
gtgaagatac tcaaccggca gaagattcgg agccttgacg tgggtgggaaa aatccgcccg gagattcaga acctgaagc  
gttcaggcac cctcacatca tcaactgta ccaggtcatc agtacacat ctgatattt catggtgatg gaatatgtct ctggaggaga  
gctatttgat tatactgta aaaatggaag gttggacgaa aaggaaagcc gccgtctgtt ccagcagatc cttccggctg  
tggattattg tcacaggcat atggtgtcc acagagattt gaaacctgag aacgtcctgc ttgatgcaca catgaatgca  
aagatagccg actttggtct tcaaacatg atgtcagatg gtgaatttt aagaacaagc tgtggctcac ccaattatgc  
cgcaccagaa gtcattcag gaagattgta cgcaggcccc gaggtggaca tctggagcag cggggtcatt ctctatgctt  
tgtgtgtgg aaccctcct ttgatgatg accatgtgcc aactctttt aagaagatat gtgatgggat cttttatacc cctcagtact  
taaaccctc agtaatcagc cttttgaaac atatgctgca ggtggatccc atgaagaggg ccgcaataaa agatatcagg  
gaacacgagt ggtttaaaca ggaccttcg aagtatctct ttctgagga cccatcttat agttcaacca tgatgatga  
cgaagcctg aaagaagtgt gtgagaagtt cgagtgttcg gaggaggagg tctcagctg cctgtacaac agaaaccacc  
aggaccact agccgtgcc taccacctca tcatagacaa caggagaata atgaatgaag ccaaagattt ctacctagca

accagccac ctgactcttt cctggacgac caccatttaa ctcggcctca ccctgaaaga gtaccgttct tgggtgccga  
aacaccacgg gcccggcaca ccctggatga attaaacca cagaaatcca aacaccaagg tgtacggaag gcaaaatggc  
atttgggaat tcgaagcaaa agccgaccca atgatatcat ggcagaagtt tntagagcaa tcaagcagtt ggattatgaa  
tggaagggtg taaacccta ttatttgcgt gtacgaagga agaactcgt gacaagcaca ttttcaaaa tgagtctaca gctataccea  
gtggatagta ggacttactt gttggatttc cgtagtattg atgatgagat tacagaagcc aatcaggga ctgctactcc  
acagagatcg ggatccatca gcaactatcg atcttgccaa aggagtgact ctgatgccga agctcaagga aagccctcag  
acgtctcct tacctcatct gtcacctccc tcgactctc cctgtgcgac gtagtccaa gaccaggaag tcatacaata gaatttttg  
aaatgtgtgc aaatctaatt aaaattcttg cacagtaa. We named *oeAmpk*.

### **Cell culture protocols**

The murine renal mesangial cells (mRMCs) were cultured in the associated cell culture medium DMEM (Dulbecco's Modified Eagle Medium) high glucose +23.75% F-12+5% FBS+14mM HEPES+1% penicillin-streptomycin. The mRMCs were maintained in the 10 cm<sup>2</sup> tissue culture flasks at 37°C, in a 5% CO<sub>2</sub> humidified atmosphere. After reaching approximately 80% confluency, the cells were treated with the control and vehicle, PA with or without 14(15)-EET. The concentration of PA and 14(15)-EET, and the culture time were presented in **Fig. 3**. DMSO (0.6%, v/v) and ethanol (0.32%, v/v) served as a control and a vehicle, respectively. The cells were harvested and prepared for western blot or qPCR analysis. All experiments were performed in triplicate noted in **Fig. 3**.

The mRMCs were transfected with 4 µg of each constructed plasmid by using Lipofectamine 2000 (Invitrogen, Carlsbad, California, USA) according to the manufacturer's instructions. The mRMCs were seeded on 6-well plates overnight prior to the transfection to ensure 90%–95% confluence for transfection. Forty-eight hours after transfection, transfected cells were treated

with Control + vehicle, and PA (300 nM) with or without 14(15)-EET (100 nM) for another 6 hours. DMSO (0.6 %, v/v) and ethanol (0.32%, v/v) served as a control and a vehicle, respectively. The cells were harvested and prepared for western blot or qPCR analysis. The mRTECs were treated with control, PA, PA with 14(15)-EET (100 nM), and PA with 14,15-DHET (100 nM), respectively, according to the similar protocols to the ones for mRMCs detailed above. All experiments were performed in triplicate as indicated.

### **Nuclear and cytoplasm protein extraction**

Nuclear and cytoplasmic protein of the treated MCs were extracted by using NE-PER nuclear and cytoplasmic extraction reagents (#78833) (Thermo Fisher Scientific) according to the manufacturer's instructions.

### **qPCR analysis**

The renal cortex tissue and harvested cells were prepared for qPCR analysis according to the manufacturer's instructions. The prepared samples were analyzed according to the methods reported previously (6). The primer sequences of target genes were presented in *SI Appendix* Table S3.

### **Western blot analysis**

The renal cortex tissue and harvested cells were prepared for immunoblot analysis of p-Ampk $\alpha$ , Pax2, p-Pax2, sEH, and Gapdh according to the manufacturer's instructions. Densitometric measurements of western blot results were conducted by using the software Image J (Image Processing and Analysis in Java). Optical density was normalized to Gapdh.

### **Statistical analysis**

Data are presented as mean  $\pm$  sem unless other noted. Statistical analyses were conducted by two-tailed *t*-test, or ANOVA followed with Tukey's (variance homogeneity) or Games-Howell's



(variance heterogeneity) post *ad hoc* comparison test using the software SPSS 22.0 (SPSS Inc., Chicago, IL) with  $P < 0.05$  as the significant level. Orthogonal partial least squares discriminant analysis (OPLS-DA) and S-plot analysis were conducted by using SIMCA 14.1 (Umetrics, Sweden).

## References

1. Rose TE, *et al.* (2010) 1-Aryl-3-(1-acylpiperidin-4-yl)urea Inhibitors of Human and Murine Soluble Epoxide Hydrolase: Structure-Activity Relationships, Pharmacokinetics, and Reduction of Inflammatory Pain. *J Med Chem* 53(19):7067-7075.
2. Liu JY, *et al.* (2009) Pharmacokinetic optimization of four soluble epoxide hydrolase inhibitors for use in a murine model of inflammation. *Brit J Pharmacol* 156(2):284-296.
3. Decleves AE, Mathew AV, Cunard R, & Sharma K (2011) AMPK mediates the initiation of kidney disease induced by a high-fat diet. *J Am Soc Nephrol* 22(10):1846-1855.
4. Liu XY, Luo Y, Zhou CY, Peng A, & Liu JY (2017) A sensitive and accurate method to simultaneously measure uric acid and creatinine in human saliva by using LC-MS/MS. *Bioanalysis* 9(22):1751-1760.
5. Wang W, *et al.* (2018) Lipidomic profiling reveals soluble epoxide hydrolase as a therapeutic target of obesity-induced colonic inflammation. *Proc Natl Acad Sci U S A* 115(20):5283-5288.
6. Luo Y, Wang L, Peng A, & Liu JY (2019) Metabolic profiling of human plasma reveals the activation of 5-lipoxygenase in the acute attack of gouty arthritis. *Rheumatology* 58(2):345-351.

**Table S1** The renal levels of lipid signaling molecules (LSMs) for the mice fed with a HFD and a CTD for 2, 4, and 8 weeks, respectively (to be continued)

LSMs (nmol/kg)	2 weeks (N = 12 each group)		4 weeks (N = 12 each group)		8 weeks (N = 11 each group)		VIP value
	CTD	HFD	CTD	HFD	CTD	HFD	
PGE <sub>2</sub>	209 ± 140	217 ± 108	357 ± 403	316 ± 214	267 ± 224	288 ± 374	1.12652
TXB <sub>2</sub>	13.2 ± 8.0	15.9 ± 7.7	12.7 ± 2.6	20.3 ± 9.4*	21.9 ± 9.5	14.9 ± 5.1*	1.00736
6-keto-PGF <sub>1α</sub>	124 ± 87	123 ± 58	116 ± 53	166 ± 82	197 ± 108	119 ± 71*	1.13624
PGF <sub>2α</sub>	99.6 ± 63.2	155 ± 69	137 ± 38	158 ± 73	232 ± 107	129 ± 52**	1.21618
19,20-DiHDPE	108 ± 49	186 ± 61**	98.3 ± 17.4	161 ± 30****	111 ± 46	131 ± 41	0.723448
17,18-DiHETE	32.4 ± 10.5	38.7 ± 4.2	32.4 ± 6.8	40.0 ± 6.6*	37.9 ± 13.2	29.6 ± 6.3	0.657003
14,15-DHET	19.0 ± 9.9	25.6 ± 8.8	16.4 ± 2.4	18.4 ± 3.9	25.7 ± 9.7	14.7 ± 3.7**	1.1105
11,12-DHET	8.2 ± 8.1	12.6 ± 8.3	6.0 ± 0.9	5.5 ± 0.9	12.1 ± 6.0	5.3 ± 2.0**	1.32076
8,9-DHET	6.8 ± 11.6	14.0 ± 12.8	3.8 ± 1.0	3.0 ± 0.8	11.4 ± 6.9	4.6 ± 2.2**	1.36589
5,6-DHET	6.0 ± 10.5	13.6 ± 13.7	3.0 ± 1.1	2.5 ± 0.8	9.7 ± 6.5	3.6 ± 1.6**	1.48676
12,13-DHOME	21.1 ± 20.6	35.6 ± 16.0	18.2 ± 4.3	21.0 ± 5.4	32.0 ± 14.3	20.6 ± 7.4*	0.898241
9,10-DHOME	15.6 ± 19.4	30.5 ± 21.5	11.4 ± 3.0	8.8 ± 2.8*	25.4 ± 14.5	13.6 ± 7.3*	1.07347
20-HETE	9.3 ± 4.3	10.2 ± 2.6	6.5 ± 1.8	9.9 ± 3.5	10.1 ± 3.4	8.8 ± 4.8	0.447059
20-COOH-ARA	73.3 ± 32.6	106 ± 46	101 ± 49	132 ± 47	117 ± 38	87.4 ± 30.5*	0.765287
15-HETE	82.0 ± 47.2	91.7 ± 32.5	67.1 ± 32.9	91.4 ± 41.2	119 ± 57	64.9 ± 39.0*	1.19335
12-HETE	642 ± 419	704 ± 43.2	747 ± 356	1175 ± 648	1452 ± 1019	973 ± 727	0.972894
11-HETE	63.4 ± 43.8	72.2 ± 32.2	51.7 ± 27.5	69.1 ± 39.0	108 ± 56	52.9 ± 34.4***	1.28373
9-HETE	49.4 ± 33.2	61.8 ± 23.6	45.7 ± 23.6	68.5 ± 30.3	77.9 ± 41.1	38.0 ± 20.8**	1.28361
8-HETE	12.5 ± 4.7	13.9 ± 3.7	8.6 ± 2.0	12.1 ± 3.2*	17.4 ± 7.9	10.8 ± 3.6	1.05944
5-HETE	41.0 ± 22.4	49.6 ± 18.2	32.7 ± 15.0	33.9 ± 7.4	54.8 ± 21.3	26.6 ± 6.3***	1.28982
6-trans-LTB <sub>4</sub>	2.9 ± 0.7	3.0 ± 0.7	3.5 ± 2.5	2.4 ± 0.4	3.3 ± 0.4	3.1 ± 1.3	0.154883
LTB <sub>4</sub>	3.1 ± 0.8	3.9 ± 0.8*	3.4 ± 1.3	3.1 ± 1.1	5.3 ± 1.6	3.6 ± 0.9*	0.787478
13(S)-HODE	360 ± 263	578 ± 188*	457 ± 335	331 ± 76	524 ± 232	400 ± 172	0.772133
9(S)-HODE	727 ± 562	1035 ± 335	824 ± 695	608 ± 167	1073 ± 491	790 ± 339	0.805402
13(S)-HOTrE	6.2 ± 3.2	11.5 ± 3.6***	8.0 ± 5.3	6.8 ± 1.4	11.5 ± 4.3	10.1 ± 4.7	0.610608
9(S)-HOTrE	4.2 ± 2.6	6.9 ± 2.7*	6.7 ± 6.5	3.7 ± 1.0	6.2 ± 2.3	4.7 ± 1.8	0.672644
13-oxo-ODE	28.7 ± 18.9	35.8 ± 6.9	27.7 ± 19.0	32.7 ± 6.6	32.9 ± 13.7	31.2 ± 9.1	0.503396
9-oxo-ODE	38.4 ± 25.5	63.0 ± 25.6*	43.2 ± 50.0	33.8 ± 6.4	46.0 ± 20.4	36.7 ± 10.5	0.66586
15-oxo-ETE	13.4 ± 8.9	18.3 ± 6.2	15.4 ± 16.8	12.8 ± 3.0	21.6 ± 11.3	10.3 ± 2.6**	1.2847
5-oxo-ETE	9.1 ± 6.6	13.4 ± 3.9	11.3 ± 16.8	9.3 ± 2.7	13.2 ± 6.3	8.1 ± 2.0*	1.03418
19(20)-EpDPA	47.9 ± 7.3	52.4 ± 12.6	48.2 ± 18.8	52.8 ± 12.0	58.2 ± 23.6	42.1 ± 9.6*	0.632085
16(17)-EpDPA	4.1 ± 1.0	4.7 ± 1.7	4.8 ± 4.7	4.4 ± 1.1	5.43 ± 2.12	3.49 ± 0.91*	0.835419
14(15)-EET	9.7 ± 2.8	10.8 ± 3.6	9.6 ± 5.5	10.8 ± 3.0	14.2 ± 6.3	8.3 ± 1.7**	1.05252
11(12)-EET	7.4 ± 1.8	8.7 ± 3.3	8.3 ± 6.6	8.5 ± 2.4	11.2 ± 5.4	6.2 ± 1.4**	1.05605
8(9)-EET	28.7 ± 5.9	32.0 ± 9.2	24.6 ± 12.2	31.6 ± 8.6	46.2 ± 20.1	24.7 ± 7.0**	1.12394
5(6)-EET	9.5 ± 2.6	11.2 ± 3.6	10.0 ± 3.7	11.8 ± 4.2	15.8 ± 7.7	8.7 ± 3.6*	1.09218
9(10)-EpOME	279 ± 200	428 ± 140*	318 ± 249	244 ± 69	454 ± 214	287 ± 127*	0.947295
12(13)-EpOME	202 ± 178	260 ± 89	187 ± 122	137 ± 35	241 ± 112	159 ± 72*	0.909739

**Table S1** The renal levels of lipid signaling molecules (LSMs) for the mice fed with a HFD and a CTD for 2, 4, and 8 weeks, respectively (to be continued)

LSMs (nmol/kg)	2 weeks (N = 12)		4 weeks (N = 12)		8 weeks (N = 11)		VIP value
	CTD	HFD	CTD	HFD	CTD	HFD	
EETs <sup>a</sup>	55.4 ± 12.4	62.6 ± 19.2	52.5 ± 26.9	29.1 ± 4.1	87.4 ± 39.0	48.0 ± 11.4**	n/a <sup>e</sup>
DHETs <sup>b</sup>	40.0 ± 40.0	65.8 ± 42.9	29.1 ± 4.6	29.5 ± 5.8	58.8 ± 28.7	28.2 ± 9.8**	n/a <sup>e</sup>
EETs + DHETs	95.4 ± 46.4	128.5 ± 49.3	81.6 ± 28.2	92.2 ± 22.0	146.3 ± 59.0	76.2 ± 15.7**	n/a <sup>e</sup>
EpOMEs <sup>c</sup>	482 ± 334	689 ± 225	505 ± 370	380 ± 99	696 ± 326	446 ± 199*	n/a <sup>e</sup>
DHOMEs <sup>d</sup>	36.8 ± 40.2	66.1 ± 37.3	29.5 ± 7.2	29.9 ± 7.7	57.4 ± 28.7	34.2 ± 14.6*	n/a <sup>e</sup>
EpOMEs+DHOMEs	518 ± 360	755 ± 248	534 ± 372	410 ± 105	753 ± 348	480 ± 209*	n/a <sup>e</sup>

Among the total of 58 LSMs in the metabolic profiling we used, the renal levels of 20 molecules were below the quantitation limitation, so here we presented the renal levels of 38 LSMs in title table. Data represent mean ± sd (N = 11 or 12). <sup>a</sup>, EETs mean the sum of 14(15)-, 11(12)-, 8(9)-, and 5(6)-EET. <sup>b</sup>, DHETs mean the sum of 14,15-, 11,12-, 8,9-, and 5,6-DHET. <sup>c</sup>, EpOMEs mean the sum of 12(13)- and 9(10)-EpOME. <sup>d</sup>, DHOMEs mean the sum of 12,13- and 9,10-DHOME. <sup>e</sup>, n/a, not applicable. In some cases, the changes in the total amount of epoxides (e.g. EETs, and EpOMEs) and their respective diol metabolites (e.g. DHETs and DHOMEs) could reflect the changes in the activity of Cyp epoxygenases. However, since the diol metabolites of epoxides (e.g. DHETs, and DHOMEs) could be further metabolized by Cyp epoxygenases and followed by sEH (Fig. 1F), the changes in either the total amount of EETs and DHETs, or the total amount of EpOMEs and DHOMEs couldn't be a reliable biomarker for the activity of Cyp epoxygenase, especially, when the total amount is decreased after a treatment. In the present study, our data suggest that the activity of Cyp epoxygenase was not increased by a HFD treatment. \*0.01 < P < 0.05, \*\*0.001 < P ≤ 0.01, \*\*\* 0.0001 < P ≤ 0.001, and \*\*\*\*P ≤ 0.0001 were determined by two-tailed *t*-test. VIP values were determined in a OPLS-DA model with SIMCA 14.1. Among the total 38 LSMs measured, 5,6-, 8,9-, and 11,12-DHET are the ones with greatest VIP values. ARA: arachidonic acid; LT: Leukotriene; PG: prostaglandin or prostacyclin; TX: thromboxane; HETE: hydroxyeicosatetraenoic acid; EET: epoxyeicosatrienoic acid; DHET: dihydroxyeicosatrienoic acid; EpOME: epoxyoctadecamonoenoic acid; DHOME: dihydroxyoctadecamonoenoic acid; EDP: epoxydocosapentaenoic acid; DiHDPE: dihydroxydocosapentaenoic acid; EpETE: epoxyeicosateteaenoic acid ; DiHETE: dihydroxyeicosateteaenoic acid; HODE: hydroxyoctadecadienoic acid; HOTrE: hydroxyoctadecadienoic acid; oxo-ETE: oxo-eicosatetraenoic acid; oxo-ODE: oxo-octadecadienoic acid.

Table S2 The renal levels of LSMs for the mice fed on a CTD, HFD, and a HFD with TPPU

LSMs (nmol/Kg)	A	B	C	A vs B	A vs C	B vs C
	(CTD)	(HFD)	(HFD + TPPU)	<i>P</i> value	<i>P</i> value	<i>P</i> value
PGE <sub>2</sub>	225 ± 196	311 ± 408	32.7 ± 19.9	0.8224	0.0312	0.1331
TXB <sub>2</sub>	25.9 ± 5.6	14.4 ± 5.5	36.9 ± 18.9	0.0006	0.2277	0.0112
6-keto-PGF <sub>1α</sub>	213 ± 113	120 ± 76	145 ± 194	0.3002	0.5153	0.9148
PGF <sub>2α</sub>	248 ± 118	125 ± 56	155 ± 230	0.1875	0.3767	0.8966
19,20-DiHDPE	129 ± 30	131 ± 45	76.3 ± 45.0	0.9910	0.0190	0.0140
17,18-DiHETE	40.8 ± 10.9	29.4 ± 6.9	44.8 ± 10.7	0.0363	0.6211	0.0038
14,15-DHET	26.9 ± 10.5	14.6 ± 4.1	11.3 ± 3.0	0.0130	<0.0001	0.1250
11,12-DHET	12.9 ± 6.2	5.7 ± 2.0	3.5 ± 1.1	0.0131	<0.0001	0.0231
8,9-DHET	12.3 ± 7.4	5.0 ± 2.2	2.1 ± 0.6	0.0313	0.0046	0.0066
5,6-DHET	10.7 ± 6.7	3.8 ± 1.7	1.3 ± 0.5	0.0254	0.0042	0.0026
12,13-DHOME	34.4 ± 14.6	21.2 ± 7.9	15.9 ± 2.8	0.0622	0.0077	0.1524
9,10-DHOME	27.7 ± 15.0	14.6 ± 7.6	6.3 ± 0.9	0.0672	0.0001	0.0191
20-COOH-ARA	111 ± 60	82.4 ± 31.2	125 ± 88	0.4019	0.9100	0.3498
15-HETE	125 ± 64	64.6 ± 42.9	21.8 ± 7.4	0.0643	0.0018	0.0289
12-HETE	1616 ± 1058	947 ± 799	82.3 ± 54.5	0.2746	0.0034	0.0188
11-HETE	115 ± 62	52.6 ± 37.9	11.5 ± 3.6	0.0386	0.0012	0.0184
9-HETE	81.5 ± 46.9	39.7 ± 22.5	6.7 ± 2.0	0.0118	< 0.0001	0.0523
8-HETE	19.1 ± 7.6	10.9 ± 3.9	6.0 ± 2.4	0.0226	0.0008	0.0119
5-HETE	65.6 ± 9.5	26.7 ± 7.0	21.2 ± 5.9	< 0.0001	< 0.0001	0.2550
13(S)-HODE	535 ± 279	390 ± 178	74.1 ± 13.9	0.2234	< 0.0001	0.0028
9(S)-HODE	1100 ± 581	772 ± 349	115 ± 42	0.3060	0.0012	0.0005
13(S)-HOTrE	11.4 ± 5.7	9.4 ± 4.2	2.0 ± 0.8	0.6681	0.0014	0.0008
9(S)-HOTrE	6.4 ± 2.4	4.7 ± 1.8	1.4 ± 0.4	0.2080	0.0003	0.0005
13-oxo-ODE	95 ± 140	30.1 ± 8.8	51.8 ± 37.3	0.3491	0.6238	0.2256
9-oxo-ODE	255 ± 426	36.0 ± 10.9	102 ± 110	0.2832	0.5326	0.1979
15-oxo-ETE	31.8 ± 7.6	10.0 ± 2.6	25.6 ± 23.7	< 0.0001	0.7184	0.1510
5-oxo-ETE	24.4 ± 16.2	7.9 ± 2.0	5.3 ± 1.7	0.0257	0.0117	0.0157
19(20)-EpDPA	68.9 ± 18.3	41.4 ± 10.1	103 ± 34	0.0025	0.0403	0.0007
16(17)-EpDPA	11.2 ± 10.2	3.4 ± 1.0	22.8 ± 17.2	0.0888	0.1926	0.0151
14(15)-EET	20.9 ± 7.6	7.9 ± 1.5	24.1 ± 9.1	0.0010	0.6771	0.0008
11(12)-EET	18.8 ± 10.5	5.8 ± 1.2	22.5 ± 9.7	0.0089	0.6913	0.0010
8(9)-EET	54.5 ± 13.6	23.0 ± 6.1	41.5 ± 14.7	< 0.0001	0.0572	0.0083
5(6)-EET	20.8 ± 5.1	8.6 ± 3.8	20.8 ± 5.1	< 0.0001	0.3359	0.0029
9(10)-EpOME	468 ± 245	279 ± 138	325 ± 98	0.1204	0.2411	0.6732
12(13)-EpOME	267 ± 95	157 ± 80	190 ± 112	0.0298	0.2498	0.7302
EETs <sup>a</sup>	115.1 ± 24.6	45.3 ± 10.3	105.5 ± 32.4	<0.0001	0.7422	<0.0001
DHETs <sup>b</sup>	62.8 ± 30.4	29.1 ± 9.7	18.2 ± 4.5	0.0172	0.0030	0.0175
EETs + DHETs	177.9 ± 24.2	74.5 ± 16.8	123.8 ± 36.3	<0.0001	0.0034	0.0051
EpOMEs <sup>c</sup>	735.6 ± 338.9	436.6 ± 216.7	515.7 ± 172.1	0.07841	0.1978	0.6448
DHOMEs <sup>d</sup>	62.1 ± 29.5	35.8 ± 15.4	22.2 ± 3.6	0.0632	0.0052	0.0521
EpOMEs+DHOMEs	797.8 ± 362.4	472.4 ± 228.0	538.0 ± 174.5	0.0716	0.1415	0.7541

Among the total of 58 LSMs in the metabolic profiling we used, the renal levels of 23 molecules were below the quantitation limitation, so here we presented the renal levels of 35 LSMs in title table. Data represent mean  $\pm$  sd (N = 10). <sup>a</sup>, EETs mean the sum of 14(15)-, 11(12)-, 8(9)-, and 5(6)-EET. <sup>b</sup>, DHETs mean the sum of 14,15-, 11,12-, 8,9-, and 5,6-DHET. <sup>c</sup>, EpOMEs mean the sum of 12(13)- and 9(10)-EpOME. <sup>d</sup>, DHOMEs mean the sum of 12,13- and 9,10-DHOME. *P* values were determined by ANOVA followed by Tukey's or Games-Howell post hoc comparison test.

**Table S3** Primer sequences for real-time quantitative PCR

Gene	Species	Forward	Reverse
<i>Pax2</i>	mouse	5'-CTTTAAGAGATGTGTCTGAGG-3'	5'-TCATTCCCCTGTTCTGATTTG-3'
<i>Ampk</i>	mouse	5'-AACGCATTTGGAGGACATGA-3'	5'-TTGTCCGGAAATCAGTGCAT-3'
<i>Il-6</i>	mouse	5'-GGACCAAGACCATCCAAT-3'	5'-ACCACAGTGAGGAATGTC-3'
<i>Ngal</i>	mouse	5'-GGCCAGTTCACTCTGGGAAA-3'	5'-TGCGAACTGGTTGTAGTCC-3'
<i>Mcp-1</i>	mouse	5'-CTTCTGGGCCTGCTGTTCA-3'	5'-CCAGCCTACTCATTGGGATCA-3'
<i>Ephx2</i>	mouse	5'-GCGTTCGACCTTGACGGAG-3'	5'-TGTAGCTTTCATCCATGAGTGGT-3'
<i>Cyp2c29</i>	mouse	5'-GCTCTCCTACTCCTGCTGAAGT-3'	5'-ATGTGGCTCCTGTCTTGCATGC-3'
<i>Cyp2c37</i>	mouse	5'-AATGGAATGGGCCTTGCA-3'	5'-GCAACGTGCTTCTTCTTGAACG-3'
<i>Cyp2c38</i>	mouse	5'-CACGGCCCATTGTTGTATTGC-3'	5'-TGAGTGTGAAACGTCTTGTCTCT-3'
<i>Cyp2c39</i>	mouse	5'-GAGGAAGCATTCCAATGGTAGAA-3'	5'-TGTGAAGCGCCTAATCTCTTTC-3'
<i>Cyp2c44</i>	mouse	5'-GCTGCCCTATACAGATGCCG-3'	5'-GTGACGCTAAGAGTTGCCCA-3'
<i>Cyp2j5</i>	mouse	5'-TCTGGGAAGCACTCCATCTCA-3'	5'-CCCTGGTGGGTAGTTTTTGG-3'
<i>Cyp2j6</i>	mouse	5'-TTAGCCACGATCTGGGCAG-3'	5'-CTGGGGGATAGTTCTTGGGG-3'
<i>Gapdh</i>	mouse	5'-AGGTCGGTGTGAACGGATTTG-3'	5'-TGTAGACCATGTAGTTGAGGTCA-3'

**Table S4** The ratio of epoxides to the respective diols in the kidneys from the mice fed with a HFD and CTD for 2, 4, and 8 weeks, respectively

Ratio	2 wks (N = 12 each)		4 wks (N = 12 each)		8 wks (N = 11 each)	
	HFD	CTD	HFD	CTD	HFD	CTD
14(15)EET/14,15-DHET	0.45 ± 0.18	0.55 ± 0.15	0.58 ± 0.10	0.58 ± 0.31	0.59 ± 0.15	0.57 ± 0.23
11(12)EET/11,12-DHET	0.89 ± 0.54	1.24 ± 0.51	1.53 ± 0.34	1.37 ± 0.93	1.30 ± 0.56	1.06 ± 0.61
8(9)EET/8,9-DHET	3.81 ± 2.59	10.0 ± 6.2**	10.8 ± 3.6	6.87 ± 2.74**	7.06 ± 4.59	5.04 ± 2.74
5(6)EET/5,6-DHET	1.51 ± 1.07	3.91 ± 2.27**	4.93 ± 1.89	3.61 ± 1.64	2.70 ± 1.13	2.14 ± 1.35
EETs/DHETs	1.22 ± 0.66	1.86 ± 0.66	2.12 ± 0.42	1.82 ± 0.83	1.84 ± 0.66	1.64 ± 0.78
12(13)EpOME/12,13-DHOME	7.80 ± 2.41	10.3 ± 6.3	6.72 ± 1.75	10.4 ± 6.6	7.70 ± 2.18	7.77 ± 3.27
9(10)EpOME/9,10-DHOME	18.5 ± 10.5	24.0 ± 14.1	28.8 ± 7.8	28.2 ± 22.3	23.4 ± 9.1	19.6 ± 7.7
EpOMEs/DHOMEs	12.1 ± 5.3	15.5 ± 7.9	13.0 ± 2.9	17.2 ± 12.5	13.4 ± 4.1	12.7 ± 5.1
19(20)EDP/19,20-DiHEDP	0.30 ± 0.11	0.53 ± 0.23**	0.33 ± 0.04	0.49 ± 0.19*	0.34 ± 0.09	0.58 ± 0.28*

Data represent mean ± sd (N = 11 or 12). In some cases, the ratio of epoxide (e.g. EET, EpOME, and EDP) to its respective diol metabolite (e.g. DHET, DHOME, and DiHEDP) could be a reference of the activity of sEH. However, since the diols could be further metabolized by Cyp epoxygenases and followed by sEH. The different diols have different metabolic stability. In addition to the sEH, microsomal EH (mEH) also mediates the metabolism of epoxide to form the corresponding diols. Therefore, the ratio of epoxide to its diol metabolite is not the reliable marker for the sEH activity in all the cases. In present study, the renal 19(20)-EDP/19,20-DiHEDP ratio reflected the activity of sEH quite well, but the renal ratio of other epoxides to their diol metabolites was not as good as the ratio of 19(20)-EDP to 19,20-DiHEDP, perhaps due to the different metabolic stability. \*0.01 < P < 0.05 and \*\*0.001 < P ≤ 0.01 were determined by two-tailed t-test.

**Table S5** The ratio of epoxides to the respective diols in the kidneys from the mice fed with a CTD, HFD, and a HFD with TPPU, respectively

Ratio	A* (CTD)	B* (HFD)	C* (HFD + TPPU)	A vs B <i>P</i> value	A vs C <i>P</i> value	B vs C <i>P</i> value
14(15)EET/14,15-DHET	1.16 ± 1.20	0.57 ± 0.16	2.12 ± 0.51	0.3144	0.0920	<0.0001
11(12)EET/11,12-DHET	2.50 ± 2.97	1.14 ± 0.45	6.40 ± 1.46	0.3617	0.0066	<0.0001
8(9)EET/8,9-DHET	7.78 ± 7.37	5.67 ± 3.34	19.4 ± 3.8	0.6957	0.0017	<0.0001
5(6)EET/5,6-DHET	4.51 ± 5.52	2.43 ± 0.80	14.3 ± 4.6	0.4920	0.0013	<0.0001
EETs/DHETs	2.83 ± 2.57	1.69 ± 0.58	5.78 ± 0.96	0.3915	0.0145	<0.0001
12(13)EpOME/12,13-DHOME	8.30 ± 2.20	7.28 ± 2.12	11.9 ± 6.2	0.5532	0.2431	0.1128
9(10)EpOME/9,10-DHOME	17.0 ± 8.5	20.3 ± 6.2	50.3 ± 11.6	0.6845	<0.0001	<0.0001
EpOMEs/DHOMEs	12.1 ± 6.0	12.3 ± 3.5	22.8 ± 6.0	0.9923	0.0001	0.0001
19(20)EDP/19,20-DiHEDP	0.57 ± 0.25	0.33 ± 0.09	1.54 ± 0.47	0.0370	0.0001	< 0.0001

\* Data represent mean ± sd (N = 10). <sup>a</sup>, EETs mean the sum of 14(15)-, 11(12)-, 8(9)-, and 5(6)-EET. <sup>b</sup>, DHETs mean the sum of 14,15-, 11,12-, 8,9-, and 5,6-DHET. <sup>c</sup>, EpOMEs mean the sum of 12(13)- and 9(10)-EpOME. <sup>d</sup>, DHOMEs mean the sum of 12,13- and 9,10-DHOME. *P* values were determined by ANOVA followed by Tukey's or Games-Howell post hoc comparison test.



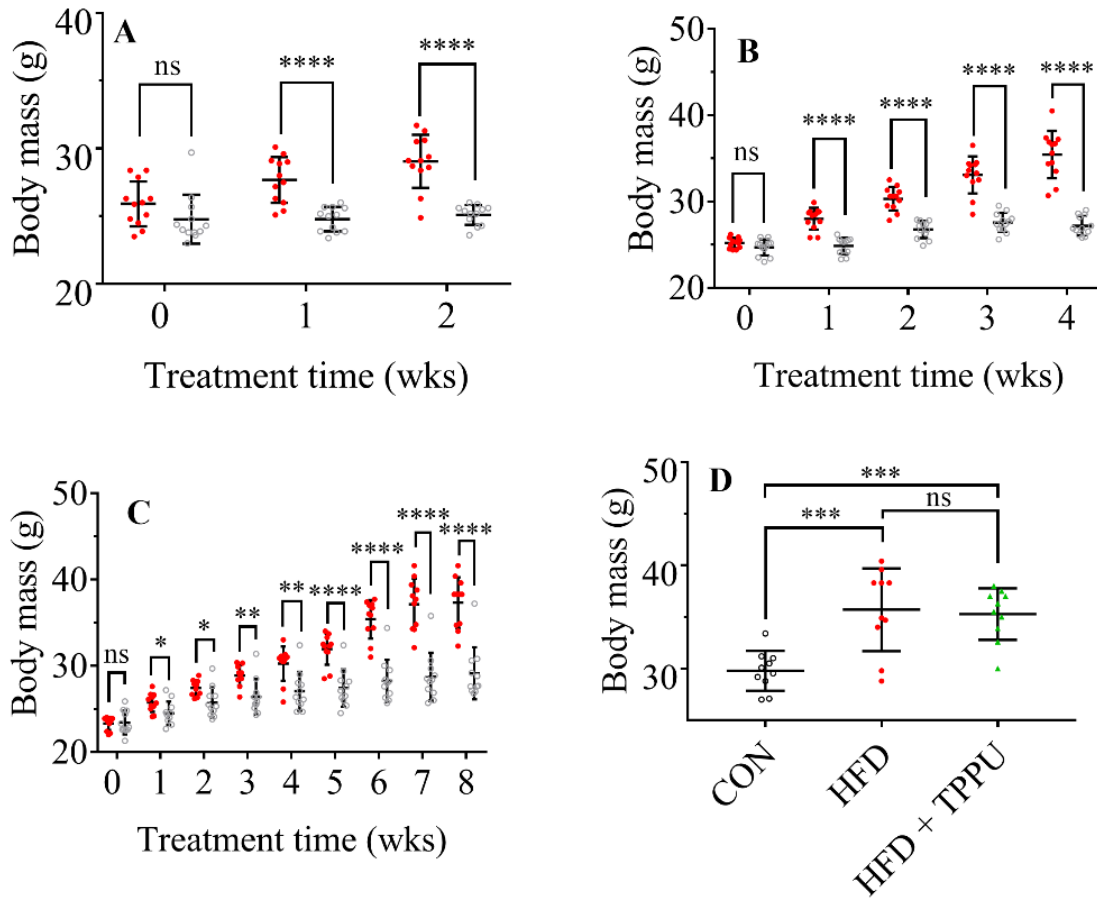


**Fig. S1** A high fat diet (HFD) significantly increased murine body mass in a time-dependent manner, and the treatment of TPPU modified HFD-induced excessive weight gain slightly. The weekly body mass for the mice fed on HFD and a CTD for 2 weeks (**A**), 4 weeks (**B**), and 8 weeks (**C**), respectively. (**D**) Treatment with TPPU slightly changed the HFD-induced excessive weight gain in this murine model. An unfilled circle, red dot, and green triangle represent the mice fed on a CTD, a HFD, and the mice fed on a HFD with TPPU, respectively. Data represent mean  $\pm$  sd (N= 10~12). \*\*\*\*,  $P \leq 0.0001$ ; \*\*\*,  $0.0001 < P \leq 0.001$ ; \*\*,  $0.001 < P \leq 0.01$ , \*  $0.01 < P < 0.05$ ; ns, no significance determined by two tailed *t*-test for (**A**), (**B**), and (**C**), and by one-way ANOVA followed by Tukey's post hoc comparison test for (**D**), respectively.

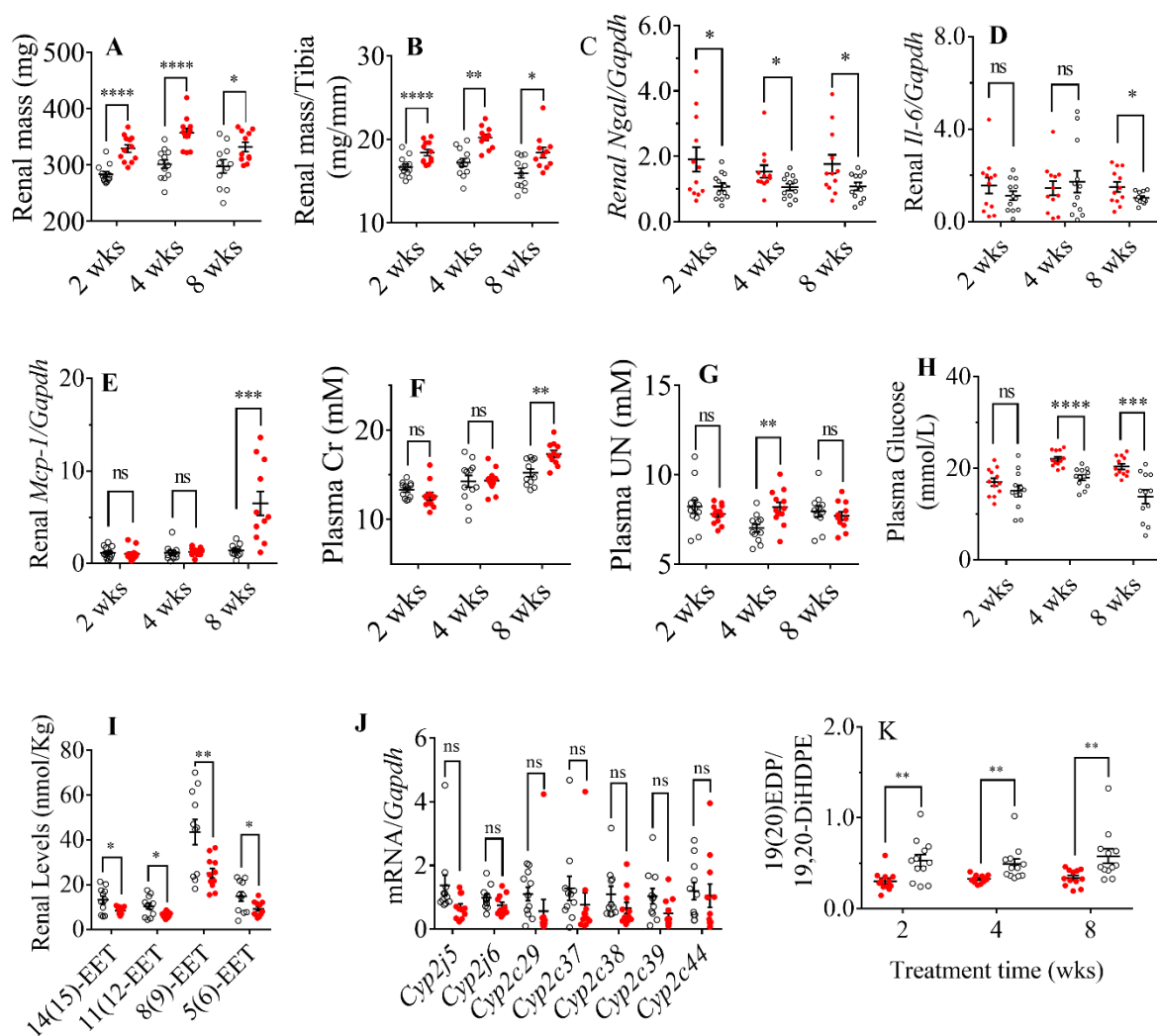


**Fig. S2** A HFD caused time-dependent renal injury in murine model. A HFD significantly increased murine renal mass (A), relative renal mass (the ratio of renal mass to tibial length (B) , and renal mRNA level of *Ngal* (C) when compared to CTD; Intake of a HFD led to time-relevant changes in renal mRNA levels of *Il-6* (D) and *Mcp-1* (E), plasma levels of Cr (F), UN (G) and glucose (H) ; (I) 8-week intake of a HFD resulted in significant decrease in renal 14(15)-, 11(12)-, 8(9)- and 5(6)-EET; (J) 8-week intake of a HFD resulted in slight changes in renal mRNA levels of *Cyp2j5*, *Cyp2j6*, *Cyp2c29*, *Cyp2c37*, *Cyp2c38*, *Cyp2c39* and *Cyp2c44*; (K) A HFD significantly decreased the renal ratio of 19(20)-EDP to 19,20-DiHDPE, suggesting that the

renal sEH activity was increased. Red dots represent the individual mouse fed with a HFD while the unfilled cycle for the individual mouse fed on a CTD. The data represent mean  $\pm$  sem (N = 11~12). ns, no significant difference ( $P \geq 0.05$ ), \*  $0.01 < P < 0.05$ , \*\*  $0.001 < P \leq 0.01$ , \*\*\*  $0.0001 < P \leq 0.001$ , and \*\*\*\*  $P \leq 0.0001$  were determined by two-tailed *t*-test.

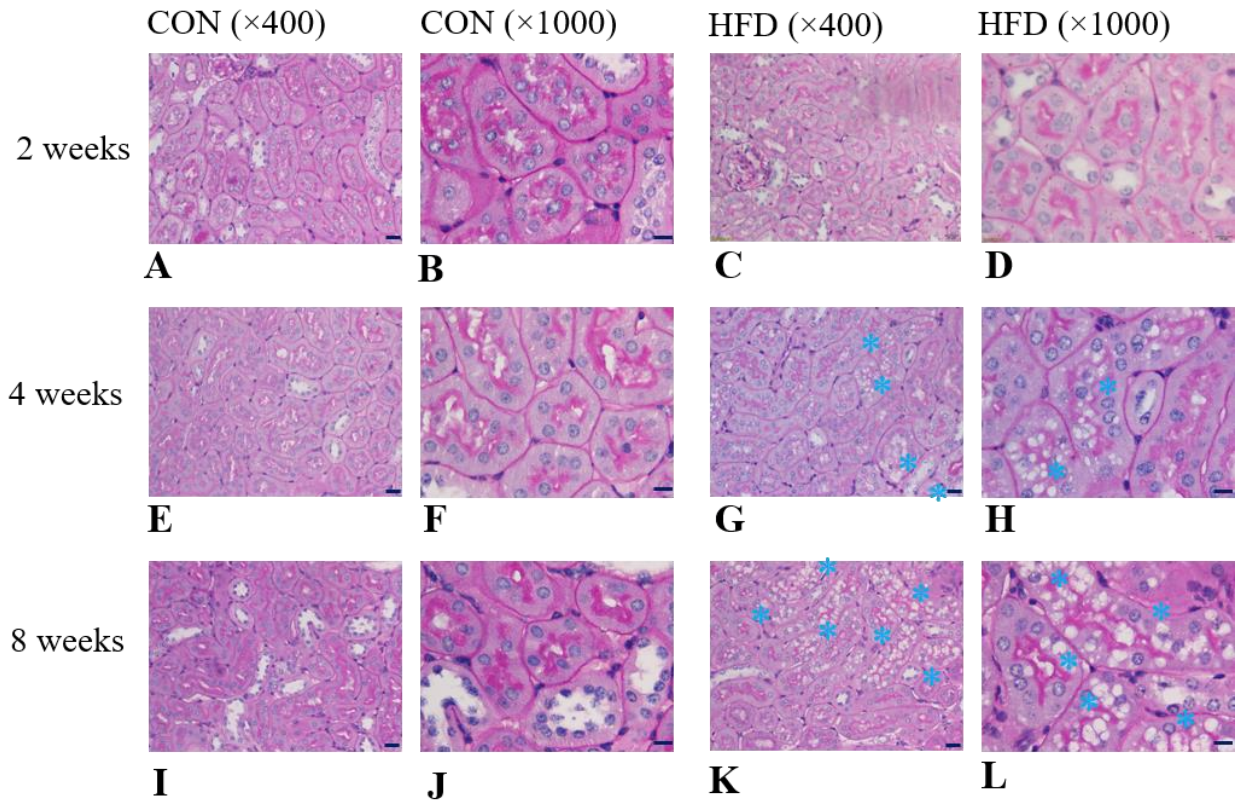


**Fig. S3** A HFD induced the accumulation of lipids in murine renal proximal tubular epithelial cells (RPTCs) time-dependently. The representative photomicrographs of renal tissue from the mice fed with a HFD and a CTD for 2, 4, and 8 weeks. Tissue slices were stained with PAS. Photomicrographs are shown at  $400\times$  and  $1000\times$  magnification. The blue asterisks indicate the vacuoles in the RPTCs. The scale marked in the right bottom corner in the  $400\times$  magnified photomicrograph represents  $20\ \mu\text{m}$  while in the  $1000\times$  magnified photomicrograph represents  $10\ \mu\text{m}$ , respectively.

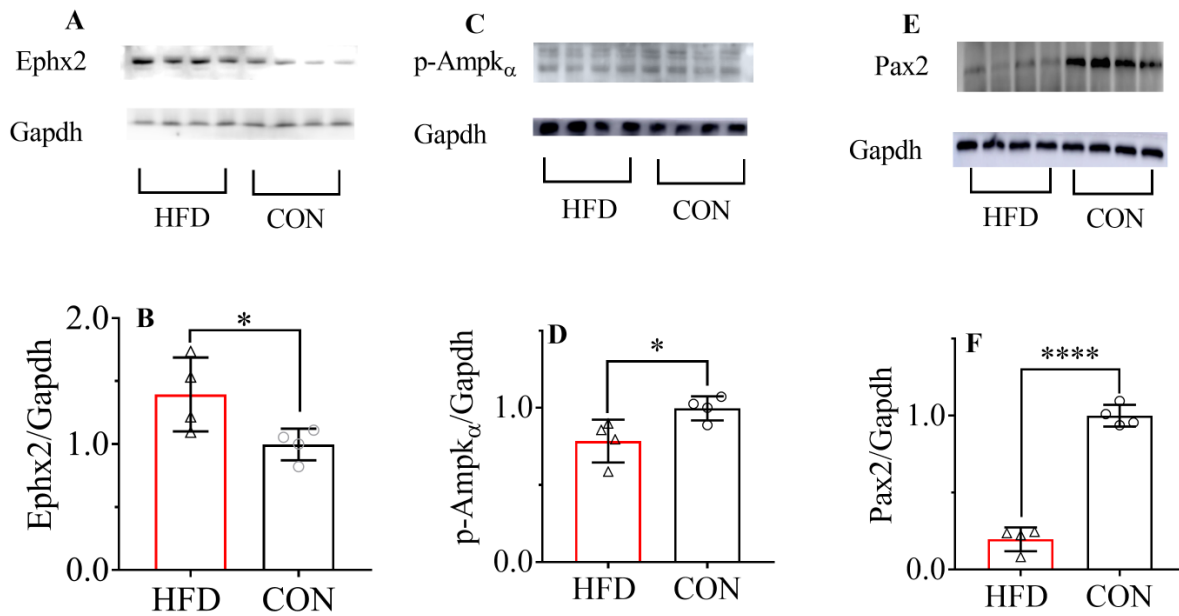


**Fig. S4** A HFD activates sEH but inactivates AMPK and PAX2 in protein levels. Western blot analysis and quantitation of the band density of Ephx2 (**A, B**), p-Ampk $_{\alpha}$  (**C, D**), and Pax2 (**E, F**) in the renal cortex from the mice fed on a HFD and a CTD for 8 weeks, respectively. Data represent mean  $\pm$  sd (N = 4). The renal tissue was selected from each group at random. \*0.01 <  $P$  < 0.05, and \*\*\*\* $P \leq 0.0001$  were determined by two-tailed  $t$ -test.

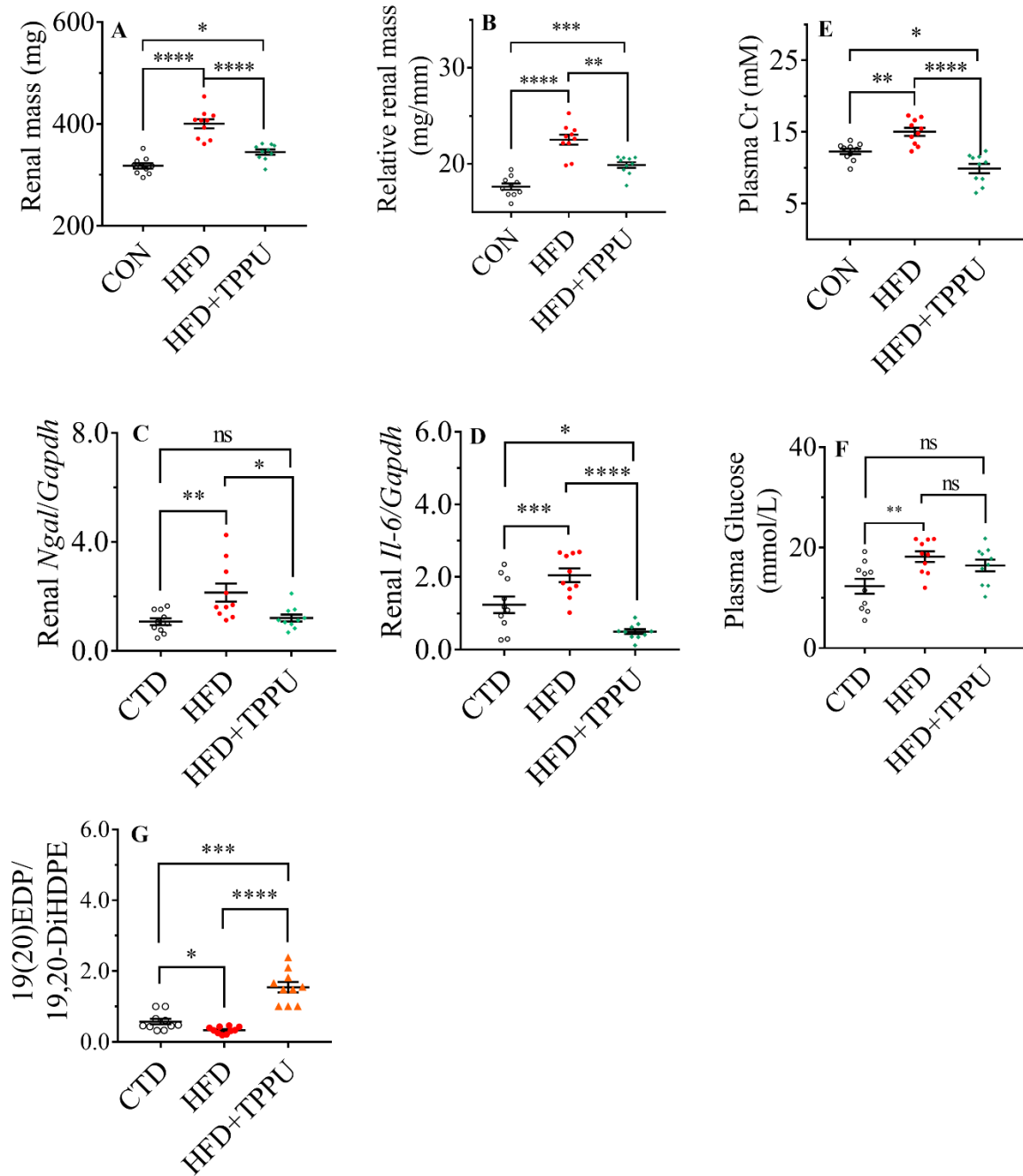


**Fig. S5** Inhibition of sEH by pharmacological intervention with a sEH inhibitor TPPU attenuated the HFD-mediated renal injury. Treatment with TPPU significantly reduced the HFD-induced increase in renal mass (A), ratio of renal mass to tibia length (B), plasma Cr (C), renal *Ngal* (D), and renal *Il-6* (E) while non-significantly decreased the HFD-induced increase in plasma glucose

(F). (G) TPPU treatment significantly increased HFD-induced decrease in the renal ratio of 19(20)-EDP to 19,20-DiHDPE, suggesting TPPU treatment significantly reversed the reduced sEH activity caused by HFD feeding. The data represent mean  $\pm$  sem (N = 10). \* $0.01 < P < 0.05$ , \*\* $0.001 < P \leq 0.01$ , \*\*\* $0.0001 < P \leq 0.001$ , and \*\*\*\* $P \leq 0.0001$  were determined by ANOVA followed by Tukey's or Games-Howell post hoc comparison test.

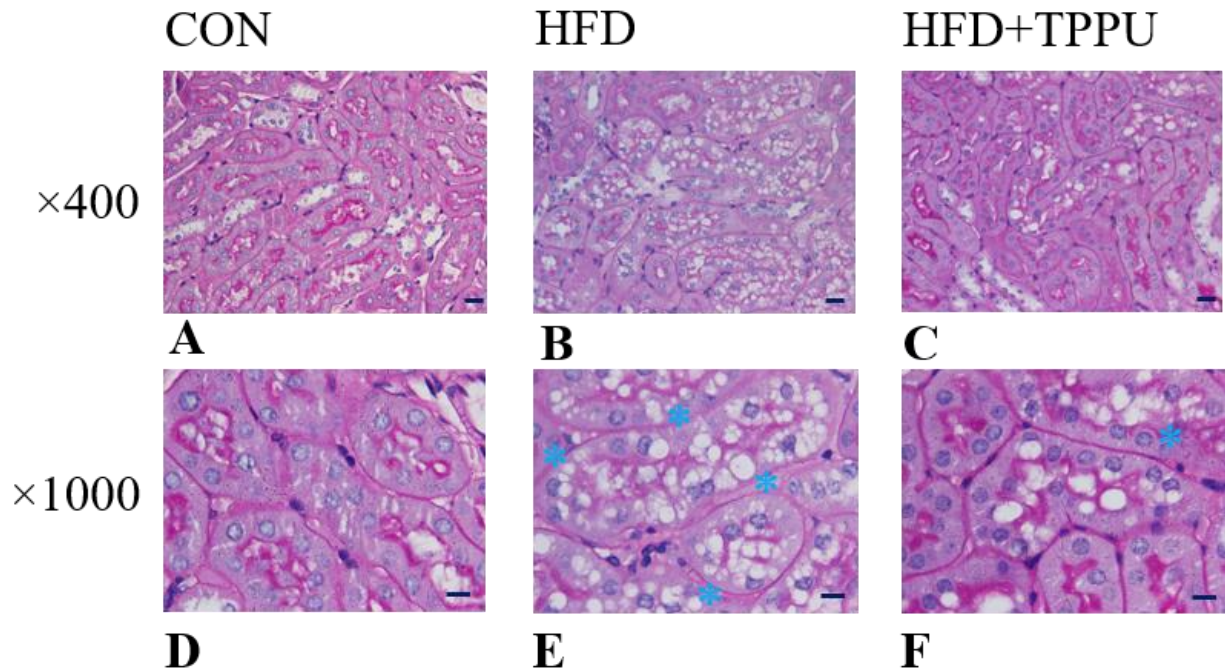


**Fig. S6** TPPU treatment attenuated the HFD-induced lipid accumulation in murine RPTCs. Tissue slices were stained with PAS. Photomicrographs are shown at 400 $\times$  and 1000 $\times$  magnification. The blue asterisks indicate the vacuoles in the RPTCs. The scale marked in the right bottom corner in the 400  $\times$  magnified photomicrograph represents 20  $\mu\text{m}$  while in the 1000  $\times$  magnified photomicrograph represents 10  $\mu\text{m}$ , respectively.



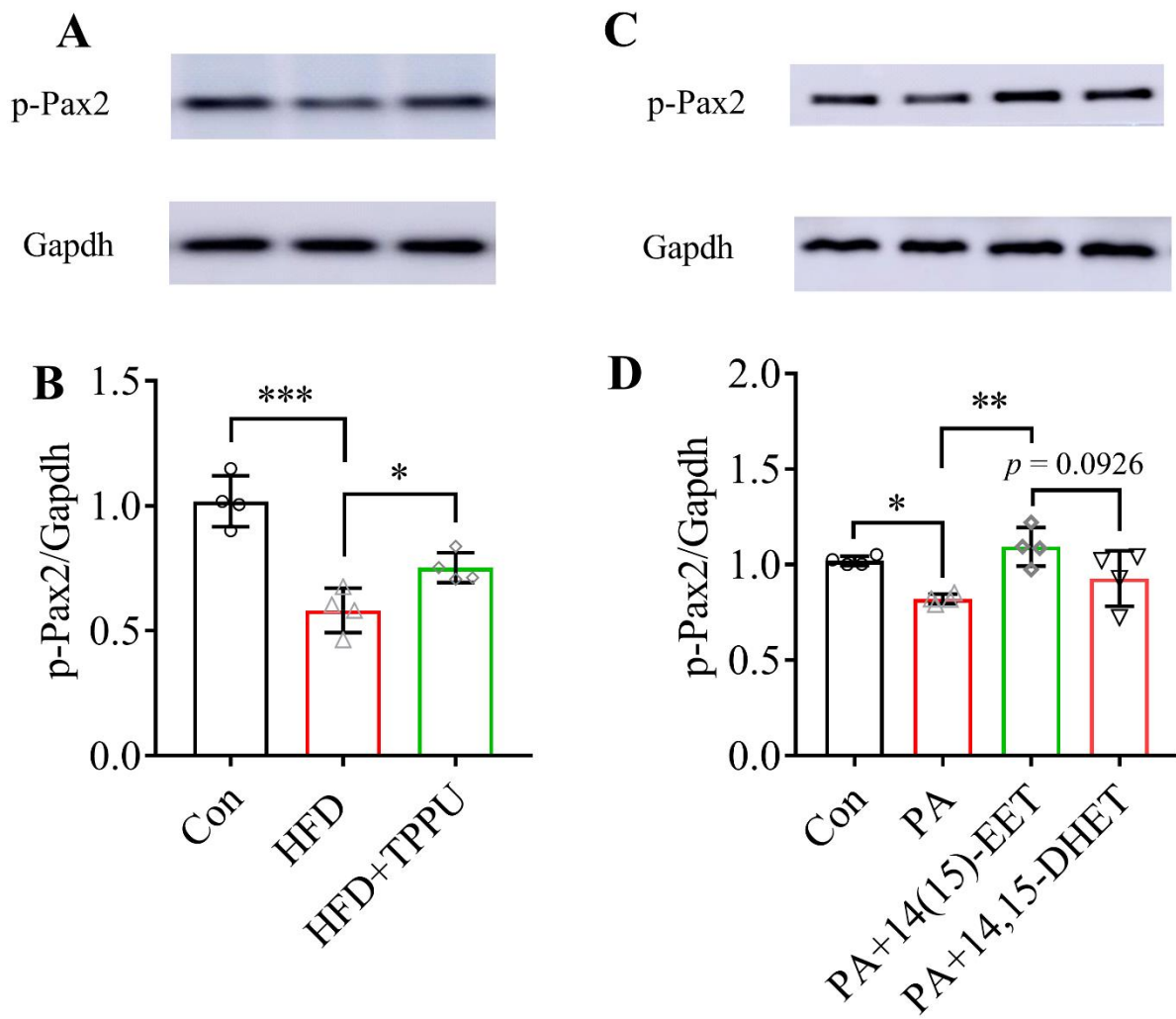


**Fig. S7** TPPU increased HFD-mediated decrease in p-Pax2 in murine kidneys and 14(15)-EET increased PA-mediated decrease in p-Pax2 in murine renal mesangial cells.

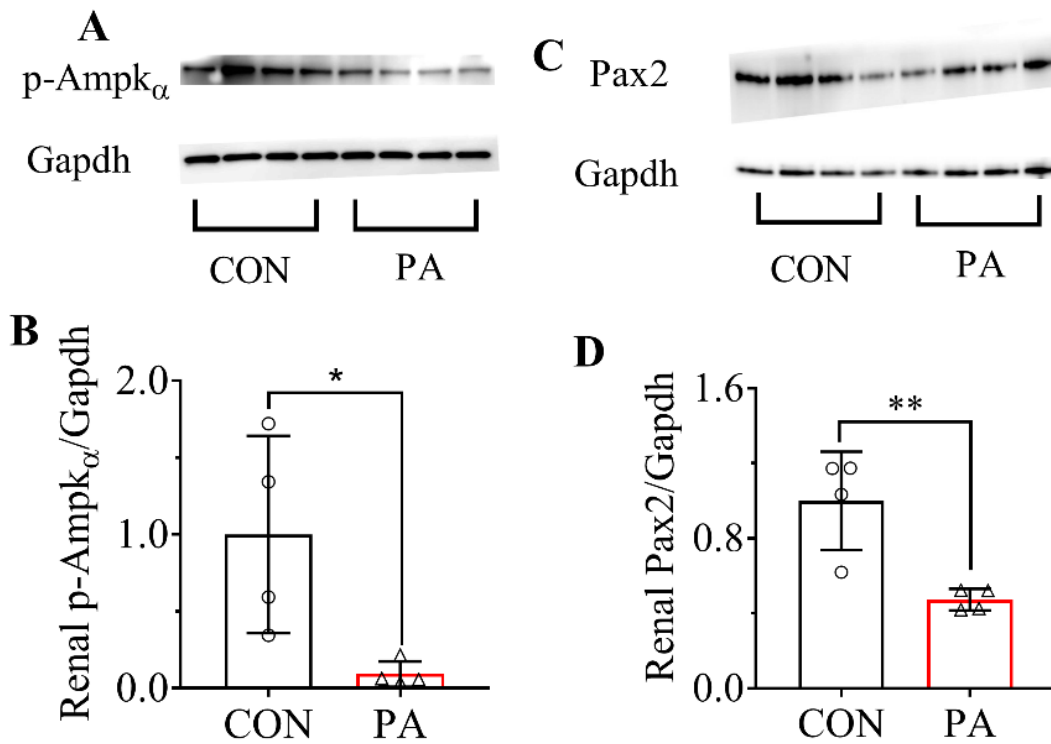


**Fig. S8** Western blot analysis and quantitation of the band density of p-Ampk $\alpha$  (A, B) and Pax2 (C, D) for the MCs treated with PA (300  $\mu$ M) for 6 hours (N = 4). Data represent mean  $\pm$  sem.

\* $0.01 < P < 0.05$ , and \*\*  $0.001 < P \leq 0.01$  were determined by two-tailed *t*-test.

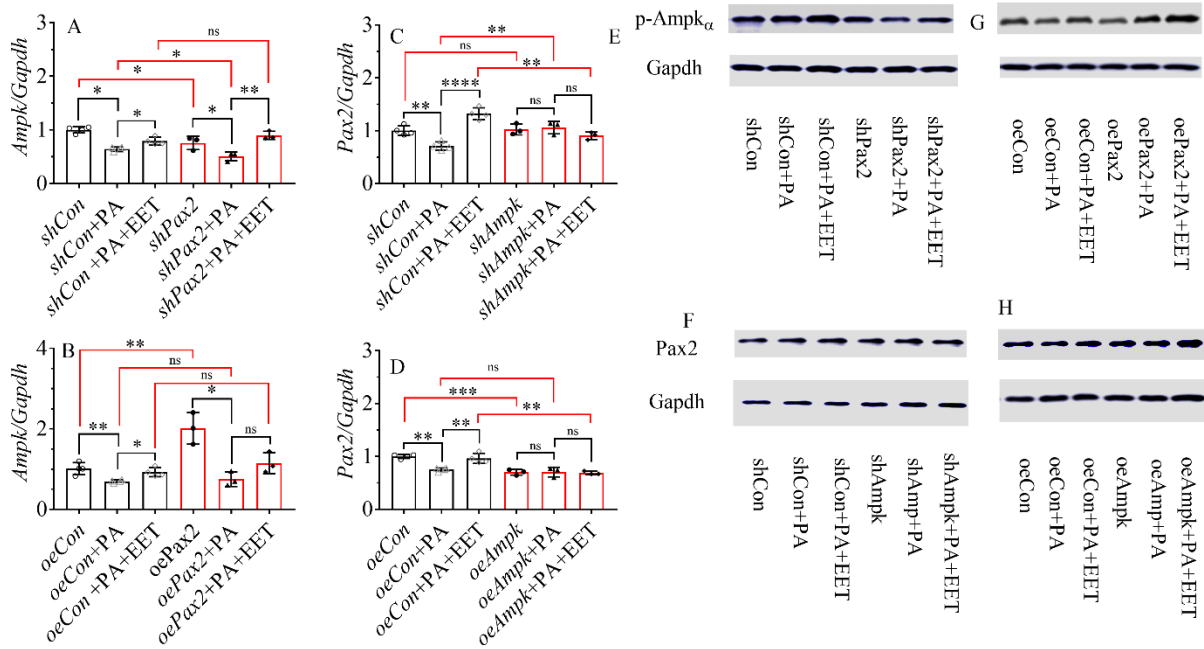


**Fig. S9** Pax2 regulates Ampk in the transfected mRMCs treated with PA with or without 14(15)-EET. The treatment of PA with or without 14(15)-EET resulted in the changes in Ampk in the mRMCs forced encoded with *shPax2* and *oePax2* at mRNA and protein levels in the similar pattern to their respective controls (**A**, **B**, **E**, and **G**). The treatment of PA with or without 14(15)-EET failed to significantly modify Pax2 at mRNA levels in the mRMCs forced encoded with *shAmpk* and *oeAmpk* (**C** and **D**), but modified protein Pax2 in the similar pattern to their respective controls (**F** and **H**). Upon the treatment of PA with or without 14(15)-EET, the forced encoding of mRMCs with *shAmpk* and *oeAmpk* resulted in slight change in protein expression of Pax2 when compared to the respective controls (**F** and **H**). Data represent mean  $\pm$  sd (n = 3 ~ 4). ns, no significant difference, \*  $0.01 < P < 0.05$ , \*\*  $0.001 < P \leq 0.01$ , \*\*\*  $0.0001 < P \leq 0.001$ , and \*\*\*\*  $P \leq 0.0001$  were determined by two-tailed *t*-test between different cells with same treatment, and by ANOVA followed by Tukey's or Games-Howell post hoc comparison test for the same cells with different treatments.

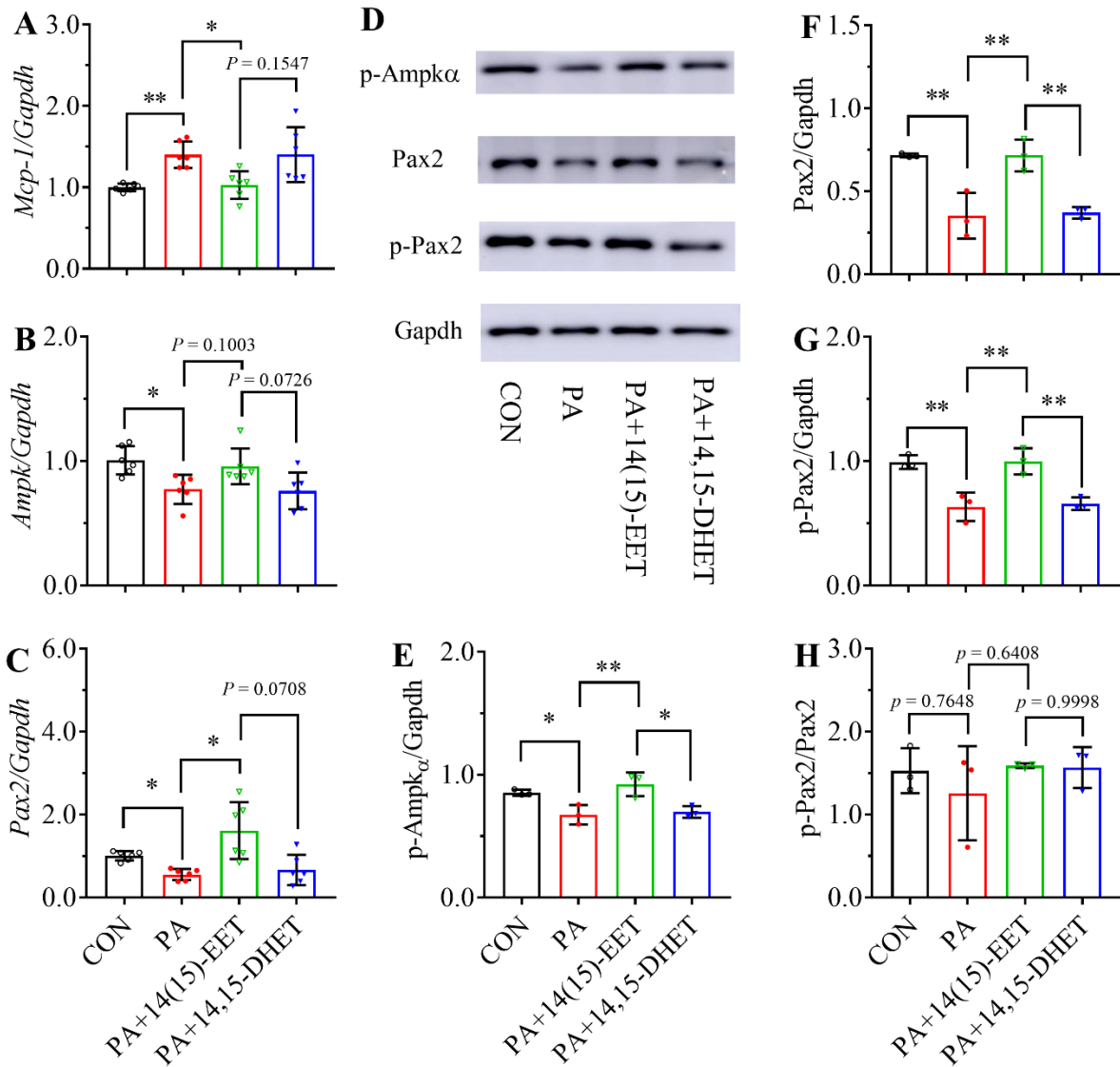


**Fig. S10** 14(15)-EET but not 14,15-DHET attenuated PA-mediated injury to murine renal tubular epithelial cells (mRTECs) by activating Ampk and Pax2. 14(15)-EET but not 14,15-DHET attenuated PA-caused increase in *Mcp-1* (A), and PA-caused decrease in *Ampk* (B) and *Pax2* (C) in the mRTECs; Western blot analysis and quantitation of the band density of p-Ampk $\alpha$  (D, E), Pax2 (D, F), and p-Pax2 (D, G), respectively. The treatment of PA, and PA with 14(15)-EET or 14,15-DHET didn't change the phosphorylation of Pax2 (H). Data represent mean  $\pm$  sd. ns, no significant difference ( $P \geq 0.05$ ), \* $0.01 < P < 0.05$ , \*\* $0.001 < P \leq 0.01$ , \*\*\* $0.0001 < P \leq 0.001$ , and \*\*\*\* $P \leq 0.0001$  were determined by ANOVA followed by Tukey's or Games-Howell post hoc comparison test.

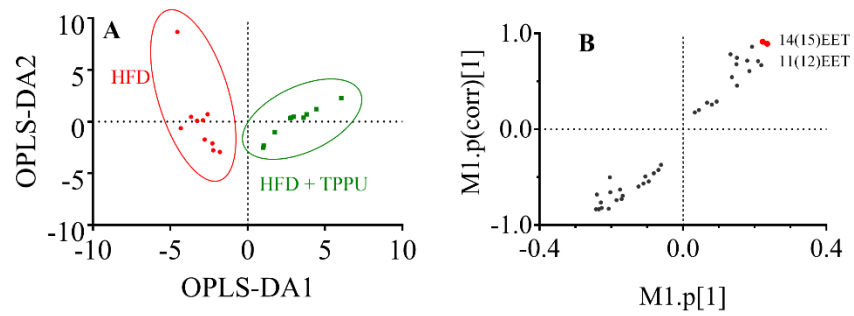


**Fig. S11** 14(15)- and 11(12)-EET are the major mediators caused by TPPU treatment to the HFD-fed mice. (A) A 2D scatter plot of OPLS-DA analysis for the renal LSMs showed visual separation of the mice fed on a HFD and a HFD with TPPU.  $R^2X=0.651$ ,  $R^2Y=0.862$ ,  $Q^2=0.728$ . (B) S-plot of the renal LSMs in an OPLS-DA model indicated that increase in renal 14(15)- and 11(12)-EET were the major mediators caused by TPPU treatment to the HFD-fed mice. The data were analyzed by using SIMCA 14.1 (Umetrics, Sweden).

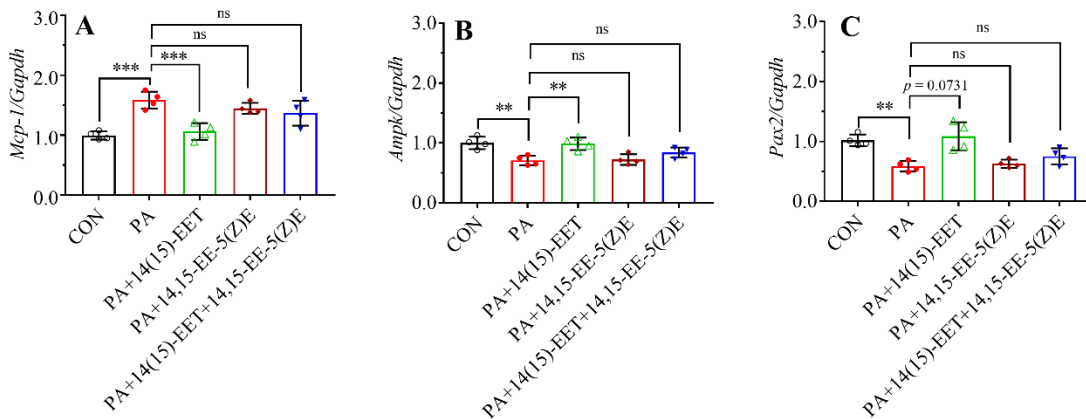


**Fig.S12** The beneficial effect of 14(15)-EET to PA-mediated mRTECs was significantly blunted by 14,15-EE-5(Z)E. 14 (15)-EET attenuated the PA-mediated increase in *Mcp-1* (**A**), decrease in *Ampk* (**B**) and *Pax2* (**C**) in mRTECs, but such beneficial effects were blunted by co-administrated with 14,15-EE-5(Z)E, an antagonist of 14(15)-EET. The concentration of 14(15)-EET and 14,15-EE-5(Z)E was 100 nM each. The data present mean  $\pm$  sd (N = 4). ns, no significant difference ( $P \geq 0.05$ ), \*\* $0.001 < P \leq 0.01$ , and \*\*\*  $0.0001 < P \leq 0.001$  were determined by ANOVA followed by Tukey's or Games-Howell post hoc comparison test.

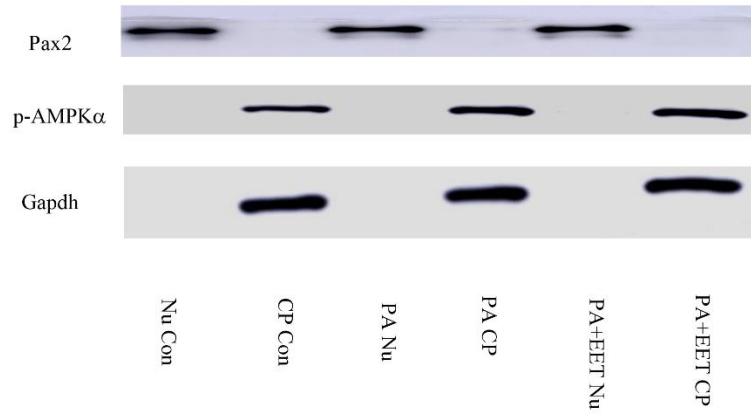


**Fig.S13** The Pax2 protein presents in the nucleus (Nu) while p-Ampk $\alpha$  presents in the cytoplasm (CP) of MCs. The expression of Gapdh demonstrated the successful separation and extraction of the protein from nucleus and cytoplasm, respectively.

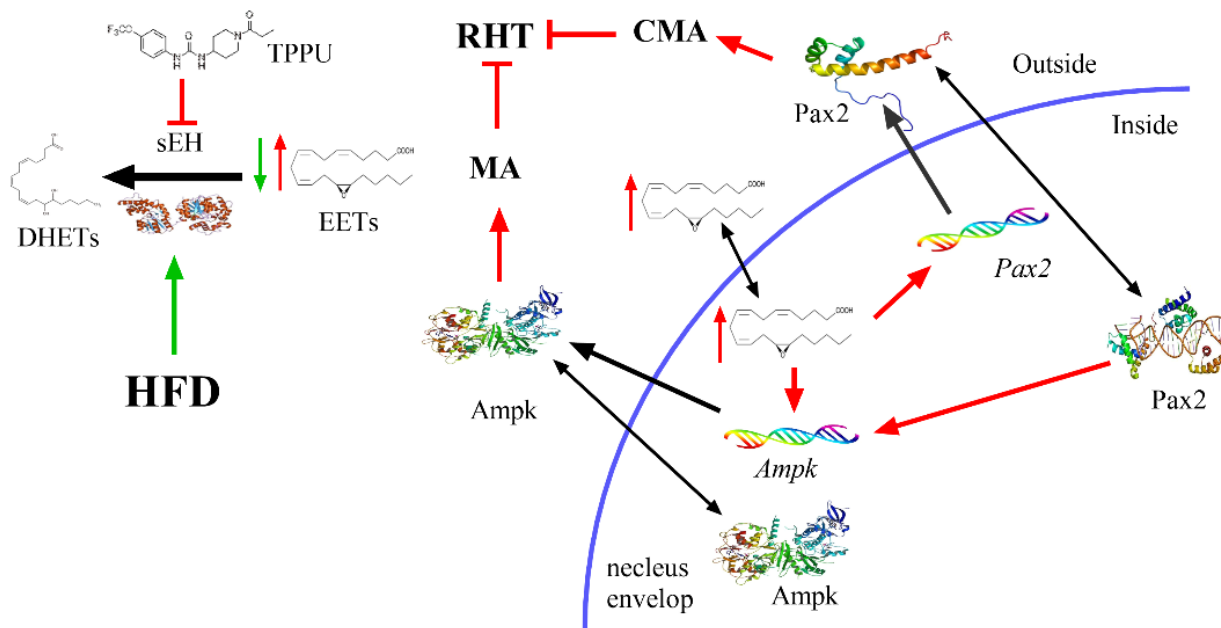


**Fig. S14** A putative mechanistic summary of the inhibition of soluble epoxide hydrolase attenuates renal injury by increased EETs activating Pax2 and Ampk in a murine model. CMA, chaperone-mediated autophagy; MA, macroautophagy; RHT, renal hypertrophy; HFD, high fat diet; sEH, soluble epoxide hydrolase; TPPU, 1-trifluoromethoxyphenyl-3-(1-propionylpiperidin-4-yl)urea; EETs, epoxyeicosatrienoic acids; DHETs, dihydroxyeicosatrienoic acids. ↑, increased or activating; ⊥ and ↓, inhibiting; ↑, activating; ↓, decreased; ↑, translational regulation; ⇅, distribution or translocation.